Engineering Transactions, **68**(3): 223–238, 2020, doi: 10.24423/EngTrans.1099.20200720
Polish Academy of Sciences • Institute of Fundamental Technological Research (IPPT PAN)
Université de Lorraine • Poznan University of Technology

Research Paper

Cattaneo-Christov Heat Flux on an MHD 3D Free Convection Casson Fluid Flow Over a Stretching Sheet

D. Gowri SHANKAR[1)], C.S.K. RAJU[2)*]
M.S. Jagadeesh KUMAR[1)], Oluwole Daniel MAKINDE[3)]

[1)] *Department of Mathematics*
VIT University, Vellore
Tamil Nadu, India

[2)] *Department of Mathematics*
GITAM School of Science, GITAM University
Bangalore, India
*Corresponding Author e-mail: rchakrav@gitam.edu, sivapdf90@gmail.com

[3)] *Faculty of Science, Stellenbosch University*
Private Bag, Saldanha, 7395-South Africa

In this investigation, we analyze the magnetohydrodynamic (MHD) three-dimensional (3D) flow of Casson fluid over a stretching sheet using non-Darcy porous medium with heat source/sink. We also consider the Cattaneo-Christov heat flux and Joule effect. The governing partial differential equations (PDEs) are transformed into ordinary differential equations (ODEs) using suitable transformations and solved by using the shooting technique. The effects of the non-dimensional governing parameters on velocity and temperature profiles are discussed with the graphs. Also, the skin friction coefficient and Nusselt number are discussed through tables. We also validate our results with the ones already available in the literature. It is found that the obtained results are in excellent agreement with the existing studies under some special cases. Our analysis reveals that the thermal relaxation parameter reduces the temperature field for the Newtonian and non-Newtonian fluid cases. It is also found that the temperature profile is decreased in the Newtonian fluid case when compared with the non-Newtonian fluid case.

Key words: MHD; Casson fluid; non-Darcy flow; Cattaneo-Christov heat flux, 3D; stretching sheet; Joule effect.

1. Introduction

The boundary layer flow of a non-Newtonian incompressible fluid over a stretching sheet has various engineering and manufacturing industry applications such as extrusion of a polymer sheet from a dye, paper production, drawing of

plastic film, etc. KHAN *et al.* [1] studied the homogeneous-heterogeneous reaction of Casson fluid. Solution for time fraction free convective flow of Casson fluid with Wright function was discussed by ALI *et al.* [2]. PRASAD *et al.* [3] considered the flow of post-stenosis dilatations effects on the couple stress fluid through stenosed arteries. RAJU and SANDEEP [4] studied the MHD Casson slip flow over a moving wedge with heat source and sink. A 3D Casson fluid flow over a stretching surface with convective boundary condition was investigated by MAHANTA and SHAW [5]. MERNONE *et al.* [6] studied a mathematical model of the peristaltic flow of a Casson fluid. NADEEM *et al.* [7] considered the 3D MHD flow of Casson fluid over a stretching sheet with a porous medium. HAN *et al.* [8] analyzed the heat transfer and flow of viscoelastic fluid using the Cattaneo-Christov heat flux model and concluded that non-Fourier's heat flux controls the flow. The influence of the Cattaneo-Christov heat flux model on the flow of variable thermal conductivity was discussed by HAYAT *et al.* [9]. STRAUGHAN [10] studied the Cattaneo-Christov model with thermal convection. IMTIAZ *et al.* [11] dealt with analysis of thermal relaxation time in the third grade fluid flow, they analyzed thermal relaxation time by using the Cattaneo-Christov heat flux model and discussed effects of chemical reaction. RAJU *et al.* [12] discussed the MHD Casson fluid past a moving wedge filled with gyrotactic microorganisms. CIARLETTA and STRAUGHAN [13] analyzed the Cattaneo-Christov equations for structural stability and uniqueness. The Cattaneo-Christov heat conduction model applied to an incompressible fluid was discussed by TIBULLO and ZAMPOLI [14], and the uniqueness of such a solution was proven. RAJU and SANDEEP [15] studied the 3D unsteady flow of Casson-Carreau fluid over a stretching sheet.

Nowadays, research on energy transfer has become a significant issue for industries and designing of materials. As a result, several authors have studied various types of mechanisms to improve the energy transfer. Among those mechanisms are Cattaneo-Christov heat flux, convective conditions, Fourier's flux, Joule heating, etc. Here, we briefly discuss some of those studies [16–31]. The influence of wall properties, heat transfer and slip conditions on MHD peristaltic transport was discussed by SRINIVAS *et al.* [16]. SIVASANKARAN and HO [17] considered MHD convection effect of temperature-dependent properties on water near its density maximum in a square cavity. The MHD mixed convection flow of micropolar liquid due to nonlinear stretching surface with convective condition was discussed by WAQAS *et al.* [18]. HSIAO [19] studied an MHD mixed convective heat transfer problem of a viscoelastic fluid past a wedge with porous suction or injection. SRINIVAS and KOTHANDAPANI [20] discussed the effect of heat and mass transfer on MHD peristaltic flow through a porous space with compliant walls. Thermal radiation effects on MHD micropolar fluid flow over a stretching sheet with variable thermal conductivity [21] were discussed by Mah-

moud. Ishak *et al.* [22] considered the MHD mixed convection stagnation point flow towards a vertical surface towards a vertical sheet immersed in a micropolar fluid. Ferrofluid fluid flow of a stagnation point of a stretching surface discussed by Prasad *et al.* [23]. Tamoor *et al.* [24] investigated the Newtonian the MHD flow of Casson liquid over a stretched cylinder moving with linear velocity. The MHD flow in the presence of non-uniform heat source/sink with thermal radiation was discussed by Upadhya *et al.* [25]. The authors [26–31] considered the non-Fourier's heat flux convective conditions with 2D and 3D flow with various physical boundary conditions.

Motivated by the above studies, in this investigation we explore the MHD 3D Casson fluid past a stretched sheet with heat source or sink. In the current work, it is of particular interest to examine the Cattaneo-Christov heat flux model. Governing non-linear momentum and energy equations are transformed into dimensionless forms and are solved numerically by the Runge-Kutta shooting scheme.

2. Mathematical formation

We consider an incompressible 3D Casson fluid past a stretching sheet with heat generation or absorption. To improve heat transport phenomena, we also consider the Cattaneo-Christov heat flux and Joule heating. It is assumed that the sheet is stretched along the xy-plane, while the fluid is placed along the z-axis. Moreover, it is assumed that the constant magnetic field is applied normal to the fluid flow, and the induced magnetic field is assumed to be negligible. Here we assumed that the sheet has stretched with the linear velocities $u = ax$ and $v = by$ along the xy-plane, respectively. The boundary layer equations of 3D

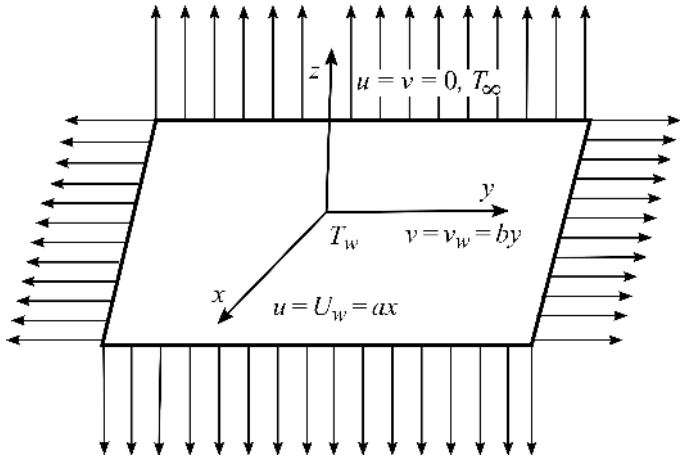

Fig. 1. Flow geometry.

incompressible Casson fluid are stated as follows (see NADEEM *et al.* [7] and PRASAD *et al.* [23]):

$$\frac{\partial u}{\partial x}+\frac{\partial v}{\partial y}+\frac{\partial w}{\partial z}=0, \tag{2.1}$$

$$u\frac{\partial u}{\partial x}+v\frac{\partial u}{\partial y}+w\frac{\partial u}{\partial z}-\upsilon\left(1+\frac{1}{\beta}\right)\frac{\partial^2 u}{\partial z^2}+\frac{\sigma B_0^2 u}{\rho}+\frac{c_b}{\sqrt{k}}u^2 + \frac{\upsilon}{k}\left(1+\frac{1}{\beta}\right)u-g\beta_T\left(T-T_\infty\right)=0, \tag{2.2}$$

$$u\frac{\partial v}{\partial x}+v\frac{\partial v}{\partial y}+w\frac{\partial v}{\partial z}-\upsilon\left(1+\frac{1}{\beta}\right)\frac{\partial^2 v}{\partial z^2}+\frac{\sigma B_0^2 v}{\rho}+\frac{c_b}{\sqrt{k}}v^2 + \frac{\upsilon}{k}\left(1+\frac{1}{\beta}\right)v-g\beta_T\left(T-T_\infty\right)=0 \tag{2.3}$$

$$\begin{aligned} u\frac{\partial T}{\partial x}+v\frac{\partial T}{\partial y}+w\frac{\partial T}{\partial z}+\lambda_1\Bigg[&u\left(\frac{\partial u}{\partial x}+\frac{\partial u}{\partial y}+w\frac{\partial u}{\partial z}\right)\frac{\partial T}{\partial x} \\ &+v\left(\frac{\partial v}{\partial x}+v\frac{\partial v}{\partial y}+w\frac{\partial v}{\partial z}\right)\frac{\partial T}{\partial y}+w\left(\frac{\partial w}{\partial x}+v\frac{\partial w}{\partial y}+w\frac{\partial w}{\partial z}\right)\frac{\partial T}{\partial z} \\ &+u\frac{\partial v}{\partial x}\frac{\partial T}{\partial x}+2uv\frac{\partial^2 T}{\partial x\partial y}+2vw\frac{\partial^2 T}{\partial z\partial y}+2wu\frac{\partial^2 T}{\partial z\partial x}\Bigg] \\ &+\lambda_1\left(u^2\frac{\partial^2 T}{\partial x^2}+v^2\frac{\partial^2 T}{\partial y^2}+w^2\frac{\partial^2 T}{\partial z^2}\right) \\ &=\alpha\frac{\partial^2 T}{\partial z^2}+Q_0\left(T-T_\infty\right)+\frac{\sigma B_0^2}{\rho c_p}\left(u^2+v^2\right), \end{aligned} \tag{2.4}$$

where u, v, and w denote the velocities in the x-, y-, and z-direction, respectively. β is the Casson fluid parameter, σ is the electrical conductivity, ρ is the fluid density, k is the permeability coefficient, g is the acceleration due to gravity, β_T is the thermal expansion coefficient, λ_1 is thermal relaxation coefficient, α is the thermal diffusivity and Q_0 is heat generation parameter. The associated boundary conditions of Eqs (2.2), (2.3), and (2.4) are as follows:
with boundary condition:

$$\begin{aligned} &u=u_w=ax, \quad v=v_w(x)=by, \quad k_f\frac{\partial T}{\partial z}=-h_f(T-T_w), && \text{at} \quad z=0, \\ &u\to 0, \quad v\to 0, \quad T\to T_\infty && \text{at} \quad z\to\infty. \end{aligned} \tag{2.5}$$

In the above equation, a and b are positive constants with time inverse unit (i.e. 1/s) associated with stretching velocities along x- and y-direction, respectively,

$$\zeta = (a/\upsilon)^{0.5} z, \quad \theta(\zeta) = \frac{T - T_\infty}{T_w - T_\infty}, \tag{2.6}$$
$$u = axf', \quad v = byg', \quad w = -(a\upsilon)^{0.5}(f + cg).$$

By using Eq. (2.6), Eqs (2.1)–(2.4) are transformed into

$$\left(1 + \frac{1}{\beta}\right) f''' - \left(M + K\left(1 + \frac{1}{\beta}\right)\right) f' - (1 + F) f'^2 + (f + g) f'' + \lambda\theta = 0, \tag{2.7}$$

$$\left(1 + \frac{1}{\beta}\right) g''' - \left(M + K\left(1 + \frac{1}{\beta}\right)\right) g' - (1 + F) g'^2 + (f + g) g'' + \lambda\theta = 0, \tag{2.8}$$

$$\frac{1}{\mathrm{Pr}}\theta'' + Q_H\theta - (f + g)\theta' + \delta\left((f + g)^2\left(f' + g'\right)\right)\theta' + (f + g)^2\theta'' + M\mathrm{Ec}\left(f'^2 + g'^2\right) = 0, \tag{2.9}$$

and the transformed boundary conditions are

$$\begin{aligned} &f = 0, \quad f' = 1, \quad g = 0, \quad g' = 1, \quad \theta' = -\mathrm{Bi}(1 - \theta), && \text{at} \quad \eta = 0, \\ &f' = 0, \quad g' = 0, \quad \theta = 0, && \text{as} \quad \to \infty, \end{aligned} \tag{2.10}$$

$M = \sigma B_0^2/\rho a$ is the magnetic field, $K = k_0^2/\rho a$ is the porosity, $F = C_b u_w/a\sqrt{K}$ is the non-Darcy flow, $\mathrm{Ec} = u_w^2/C_p\left(T_w - T_\infty\right)$ is the Eckert number, $\lambda = g\beta_T u_w/\rho a$ is thermal buoyancy, $\delta = \lambda a/\rho$ is the thermal relaxation, $\mathrm{Pr} = \mu c_p/k$ is the Prandtl number, $Q_H = Q_0/\rho a$ is the heat source or sink, and $\mathrm{Bi} = h_f/k_f a$ is the Biot number.

Distinctive measures of practical attention are the skin friction coefficient and local Nusselt number which are defined as

$$\mathrm{Nu}_x = \frac{xq_w}{k\left(T_\infty - T_w\right)} \quad \text{and} \quad C_f = \frac{\tau_w}{\rho U_w^2}. \tag{2.11}$$

Using the non-dimensional variables, we obtain

$$\begin{aligned} \sqrt{\mathrm{Re}_x}\, C_{fx} &= \left[\left(1 + \frac{1}{\beta}\right) f''(\zeta)\right]_{\zeta=0}, \\ \sqrt{\mathrm{Re}_x}\, C_{fy} &= \left[\left(1 + \frac{1}{\beta}\right) g'(\zeta)\right]_{\zeta=0}, \\ \mathrm{Nu}_x &= -\mathrm{Re}_x^{0.5}\,\theta'(0), \end{aligned} \tag{2.12}$$

where $\mathrm{Re}_x = \left(\frac{xu_w(x)}{\upsilon}\right)$ is the local Reynolds number.

3. Results and discussion

To validate the physical model, the numerical solutions for the dimensionless velocity and temperature as well as the local Nusselt number and friction factor coefficients are presented using graphs and tables for various values of physical parameters for both the Newtonian and non-Newtonian flow cases. For numerical solutions, we have chosen the non-dimensional parameter values Bi $= 0.3$, $Gr = 0.1$, $K = 0.5$, $\beta = 0.5$, $\gamma = 0.2$, $Q_H = 0.1$, $\lambda = 0.2$, $M = 0.2$, $\delta = 0.1$, Pr $= 0.72$, Ec $= 0.2$. These numeric values are used throughout the entire study apart from the variations in the corresponding figures and tables. In this study, the graphs with solid and dashed lines indicate the Newtonian and non-Newtonian flow cases, respectively.

Figures 2–17 demonstrate the variations of velocity, temperature and concentration profiles for different values of K, Q_H, γ, M, λ, Ec, and Bi. The effects of Biot number on the velocity and temperature profiles are shown in Figs 2–4. It is clear that the higher values of Bi improve the velocity profiles as well as temperature profiles. It is interesting to mention that the influence of Bi is strong in the non-Newtonian flow compared with the Newtonian flow. Due to the domination of viscosity in the flow we observed a mixed performance in the temperature field in the presence of the non-Newtonian flow case. The effects of Eckert number on the velocity and temperature profiles are shown in Figs 5–7. It is clear that the higher values of Ec improve the velocity profiles as well as temperature profiles. It is interesting to mention that the influence of Ec is higher in the non-Newtonian flow compared with the Newtonian flow. Due to the domination of viscosity in the flow we observed a mixed performance in the temperature field in the presence of the non-Newtonian flow case. The effect of β on the velocity and temperature profiles is shown in Figs 6 and 7. It is noticed that an increasing β tends to decrease the temperature and improves the velocity fields. Generally,

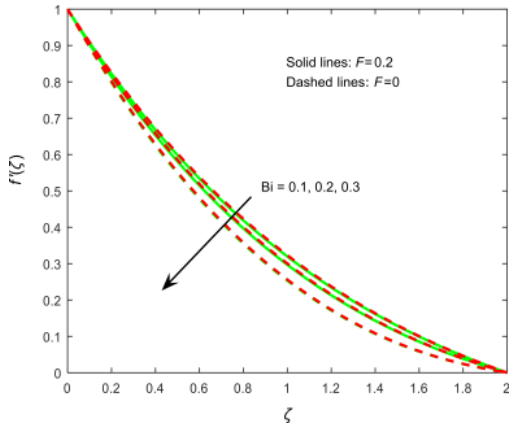

Fig. 2. Influence of Bi on $f'(\varsigma)$.

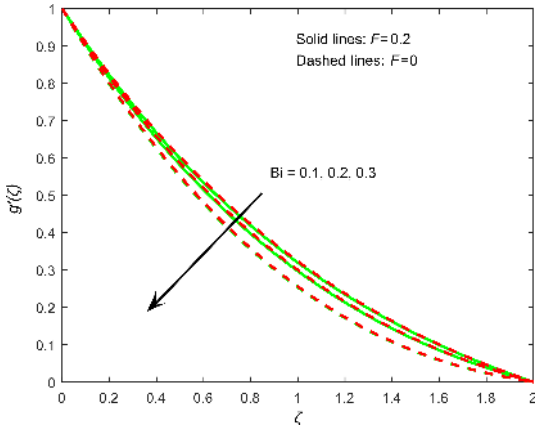

FIG. 3. Influence of Bi on $g'(\varsigma)$.

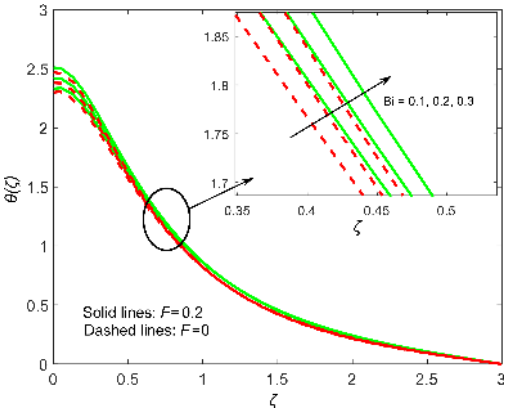

FIG. 4. Influence of Bi on $\theta(\varsigma)$.

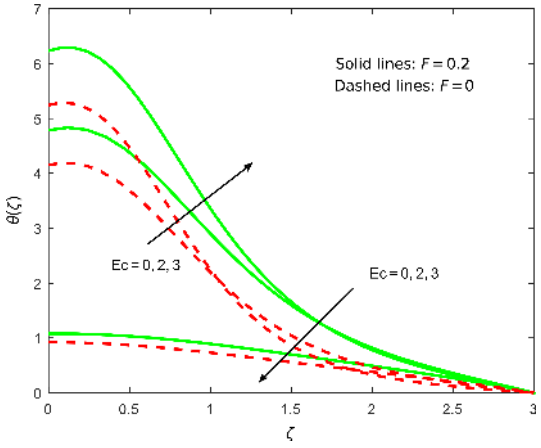

FIG. 5. Influence of Ec on $\theta(\varsigma)$.

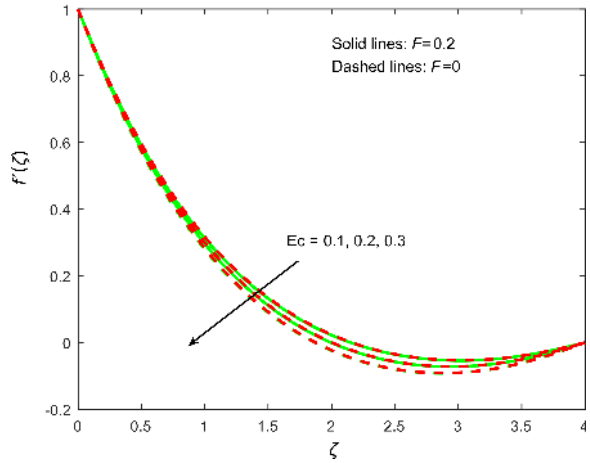

FIG. 6. Influence of Ec on $f'(\varsigma)$.

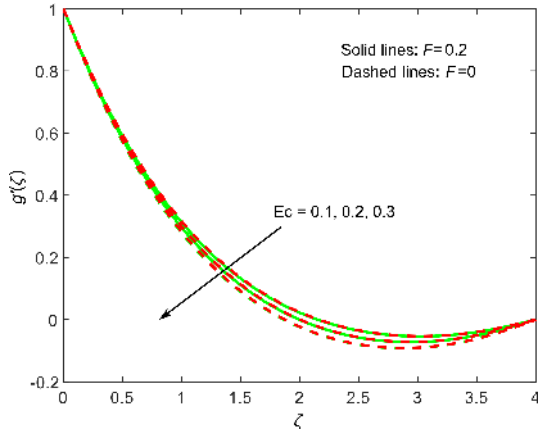

FIG. 7. Influence of Ec on $g'(\varsigma)$.

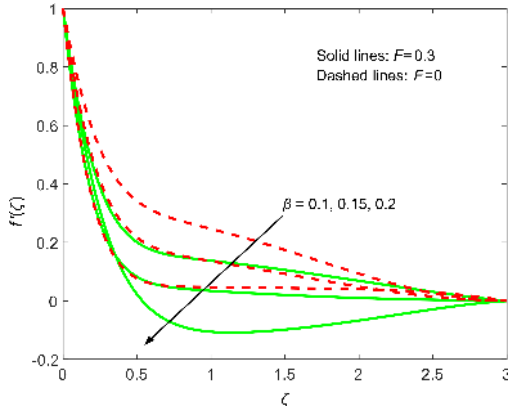

FIG. 8. Influence of β on $f'(\varsigma)$.

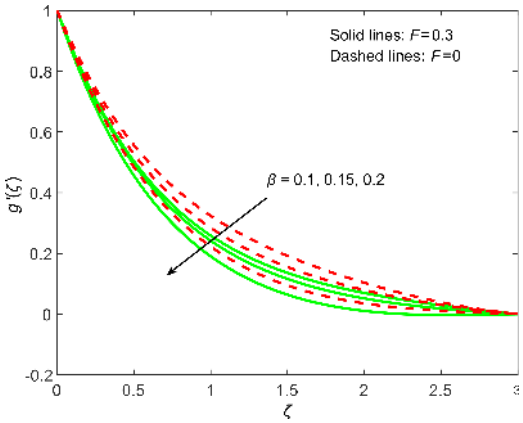

FIG. 9. Influence of β on $g'(\varsigma)$.

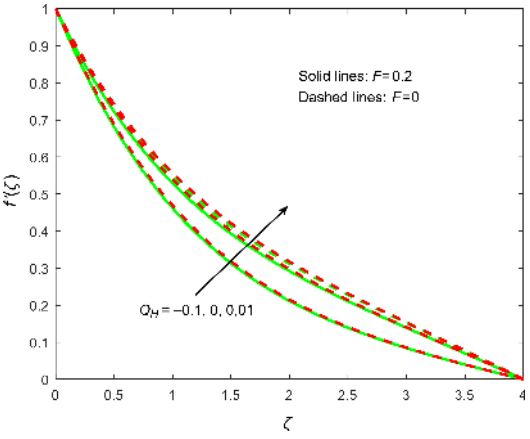

FIG. 10. Influence of Q_H on $f'(\varsigma)$.

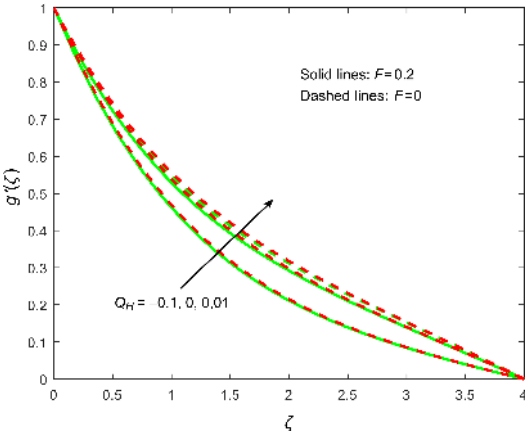

FIG. 11. Influence of Q_H on $g'(\varsigma)$.

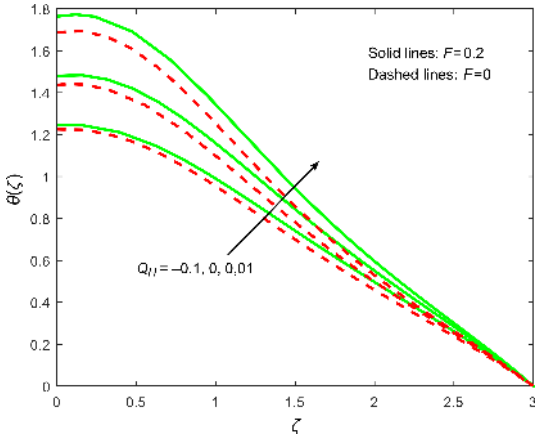

FIG. 12. Influence of Q_H on $\theta(\varsigma)$.

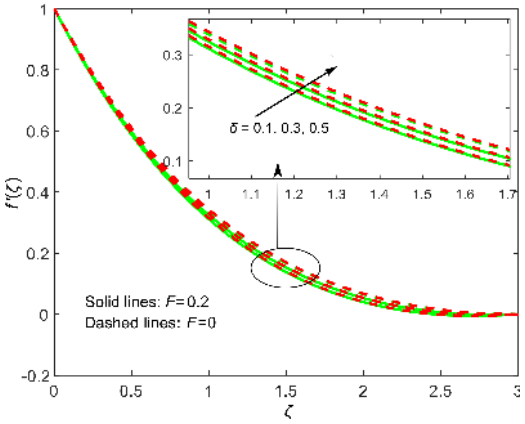

FIG. 13. Influence of δ on $f'(\varsigma)$.

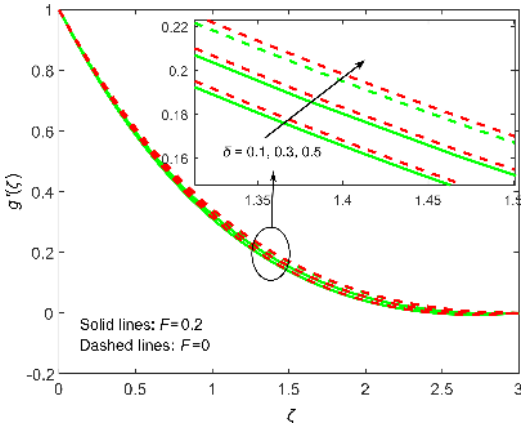

FIG. 14. Influence of δ on $g'(\varsigma)$.

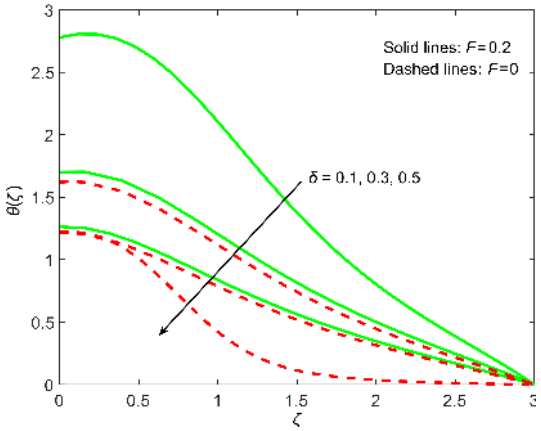

FIG. 15. Influence of δ on $\theta(\varsigma)$.

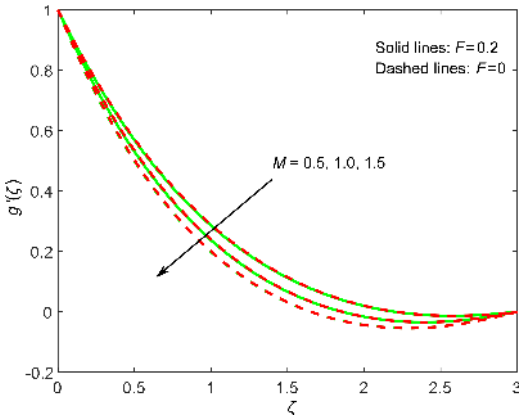

FIG. 16. Influence of M on $g'(\varsigma)$.

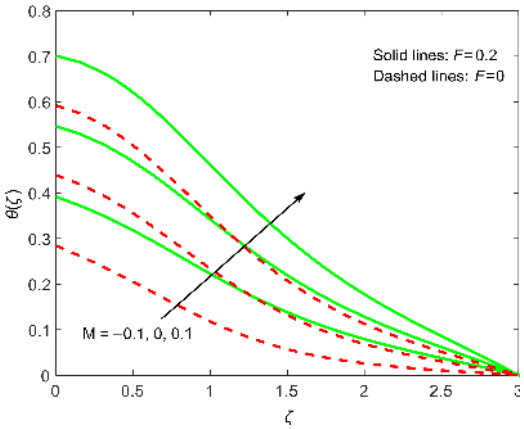

FIG. 17. Influence of M on $\theta(\varsigma)$.

increasing values of β make the neighboring particles move faster and this helps to improve the velocity fields and depreciate the temperature field. The effect of heat sources on velocity and temperature profile is shown in Figs 8–10. It is clear that the higher values Q_H improve the velocity profiles as well as temperature profiles. It is wort mentioning that the influence of Q_H is high in the non-Newtonian flow compared with the Newtonian flow. Due to the domination of viscosity nature in the flow we have seen a mixed performance in the temperature field in the presence of the non-Newtonian flow case. The effect of δ on the velocity and temperature profiles is shown in Figs 11–13. It is noticed that an increasingδ tends to decrease the temperature and improves the velocity fields. Generally, increasing values of δ make the neighboring particles move faster; this helps to improve the velocity fields and depreciate the temperature field. The effect of M velocity and temperature profile is shown in Figs 14 and 15. It is clear that an increasing M tends to decreases the temperature and improves the velocity fields. Generally, increasing values of M make the neighboring particles move faster; this helps to improve the velocity fields and depreciate the temperature field.

Table 1 displays the impact of various thermophysical governing parameters (Bi, Ec, β, Q_H, δ, and M) on the local Nusselt number and friction factor coefficient for the Newtonian and non-Newtonian flow cases. The rate of heat

Table 1. Numerical results of various values of thermophysical parameters on the skin friction coefficient and Nusselt number for the Newtonian and non-Newtonian fluid cases.

Bi	Ec	Q_H	δ	M	$\sqrt{\mathrm{Re}_x}\,C_{fx}$		$\sqrt{\mathrm{Re}_x}\,C_{fy}$		$\mathrm{Nu}_x\mathrm{Re}_x^{-1/2}$	
					$F=0$	$F=0.2$	$F=0$	$F=0.2$	$F=0$	$F=0.2$
0.1					−2.854077	−2.790527	−2.854077	−2.790527	0.608577	0.609444
0.2					−2.992621	−2.931528	−2.992621	−2.931528	1.604808	1.607563
0.3					−3.257933	−3.201625	−3.257933	−3.201625	3.513826	3.521987
	0.1				−2.928671	−2.863968	−2.928671	−2.863968	1.496625	1.498569
	0.2				−2.995842	−2.933026	−2.995842	−2.933026	1.603694	1.606636
	0.3				−3.062394	−3.001286	−3.062394	−3.001286	1.707088	1.710934
		−0.1			−2.285371	−2.202230	−2.285371	−2.202230	0.265850	0.263871
		0			−1.977179	−1.882867	−1.977179	−1.882867	−0.381569	−0.386893
		0.1			−1.900484	−1.803124	−1.900484	−1.803124	−0.545610	−0.552071
			0.1		−2.966075	−2.903026	−2.966075	−2.903026	1.685199	1.689376
			0.3		−2.901503	−2.836196	−2.901503	−2.836196	1.529119	1.530739
			0.5		−2.833342	−2.765299	−2.833342	−2.765299	1.362069	1.360108
				0.5	−3.134383	−3.074783	−3.134383	−3.074782	1.394788	1.398329
				1.0	−3.484827	−3.431805	−3.484827	−3.431805	1.611914	1.617069
				1.5	−3.790626	−3.742272	−3.790626	−3.742272	1.797771	1.803954

transfer increases with rising values of Bi, Ec, and Q_H, and the Newtonian fluid case has higher heat transfer rate than the non-Newtonian fluid case. The heat transfer rate is decreased with higher values of β, δ, and M. The friction factor is improved with Q_H and δ and reduced with Bi, Ec, and M. It is also interesting to mention that the friction factor coefficient is higher in the non-Newtonian fluid case. In Table 2, we compare the current solutions with already exiting studies under limited cases. We find that good agreement with those solutions.

Table 2. Comparison of the present results with published literature for skin friction coefficients when $Q_H = \mathrm{Bi} = \delta = \mathrm{Pr} = K = F = \mathrm{Ec} = 0$.

β	M	$\lambda = 0$		$\lambda = 0.5$			
		Nadeem *et al.* [7] C_{fx}	Present results C_{fx}	Nadeem *et al.* [7] C_{fx}	Nadeem *et al.* [7] C_{fy}	Present results C_{fx}	Present results C_{fy}
1	0	−1.4142	−1.4142	−1.5459	−0.6579	−1.5459	−0.6579
5		−1.0954	−1.0952	−1.1974	−0.5096	−1.1980	−0.5096
∞		−1.0049	−1.0050	−1.0932	−0.4653	−1.0932	−0.4653
1	10	−4.6904	−4.6904	−4.7263	−2.3276	−4.7263	−2.3275
5		−3.6331	−3.6330	−3.6610	−1.8030	−3.6610	−1.8030
∞		−3.3165	−3.3165	−3.3420	−1.6459	−3.3420	−1.6459
1	100	−14.2127	−14.2170	−14.2244	−7.1004	−14.2240	−7.1004
5		−11.0091	−11.0091	−11.0182	−5.5000	−11.0170	−5.4998
∞		−10.0490	−10.0491	−10.0580	−5.0208	−10.0581	−5.02078

4. Conclusion

The hydromagnetic boundary layer 3D flow of Casson fluid past a stretching sheet embedded in a non-Darcy porous medium with the Cattaneo-Christov heat flux and Joule heating effect was numerically examined. The effects of various thermophysical parameters on the entire flow structure and the thermal boundary layer were obtained and discussed graphically and quantitatively. It was found that the thermal relaxation parameter reduces the temperature field for the Newtonian and non-Newtonian fluid cases, and the temperature profile is smaller in the Newtonian fluid case compared with the non-Newtonian fluid case. Some profiles showed asymptotic behavior due to the dominance of Joule heating and thermal convective conditions in the flow.

References

1. Khan M.I., Waqas M., Hayat T., Alsedi A., A comparative study of Casson fluid with homogeneous heterogeneous reaction, *Journal of Colloid and Interface Science*, **498**: 85–90, 2017, doi: 10.1016/j.jcis.2017.03.024.

2. Ali F., Sheikh N.A., Khan I., Saqib M., Solution with Wright function for time fraction free convective flow of Casson fluid, *Arabian Journal for Science and Engineering*, **42**: 2565–2572, 2017, doi: 10.1007/s13369-017-2521-3.

3. Prasad K.M., Sudha T., Phanikumari M.V., The effect of post-stenotic dilatations on the flow of couple stress fluid through stenosed arteries, *American Journal of Computational Mathematics*, **6**(4): 365–376, 2016, doi: 10.4236/ajcm.2016.64036.

4. Raju C.S.K., Sandeep N., MHD slip flow of a dissipative Casson fluid over a moving geometry with heat source/sink: a numerical study, *Acta Astronautica*, **133**: 436–443, 2017, doi: 10.1016/j.actaastro.2016.11.004.

5. Mahanta G, Shaw S., 3D Casson fluid flow past a porous linearly stretching sheet with convective boundary condition, *Alexandria Engineering Journal*, **54**(3): 653–659, 2015, doi: 10.1016/j.aej.2015.04.014.

6. Mernone A.V., Mazumdar J.N., Lucas S.K., A mathematical study of peristaltic transport of a Casson fluid, *Mathematical and Computer Modelling*, **35**(7–8): 895–912, 2002, doi: 10.1016/S0895-7177(02)00058-4.

7. Nadeem S., Haq R.U., Akbar N.S., Khan Z.H., MHD three-dimensional Casson fluid flow past a porous linearly stretching sheet, *Alexandria Engineering Journal*, **52**(4): 577–582, 2013, doi: 10.1016/j.aej.2013.08.005.

8. Han S., Zheng L., Li C., Zhang X., Coupled flow and heat transfer in viscoelastic fluid with Cattaneo-Christov heat flux model, *Applied Mathematics Letters*, **38**: 87–93, 2014, doi: 10.1016/j.aml.2014.07.013.

9. Hayat T., Khan M.I., Farooq M., Alsaedi A., Waqas M., Yasmeen T., Impact of Cattaneo-Christov heat flux model in flow of variable thermal conductivity fluid over a variable thicked surface, I*nternational Journal of Heat and Mass Transfer*, **99**: 702–710, 2016, doi: 10.1016/j.ijheatmasstransfer.2016.04.016.

10. Straughan B., Thermal convection with the Cattaneo-Christov model, *International Journal of Heat and Mass Transfer*, **53**(1–3): 95–98, 2010, doi: 10.1016/j.ijheatmasstransfer.2009.10.001.

11. Imtiaz M., Alsaedi A., Shafiq A., Hayat T., Impact of chemical reaction on third grade fluid flow with Cattaneo-Christov heat flux, *Journal of Molecular Liquids*, **229**: 501–507, 2017, doi: 10.1016/j.molliq.2016.12.103.

12. Raju C.S.K., Hoque M.M., Sivasankar T., Radiative flow of Casson fluid over a moving wedge filled with gyrotactic microorganisms, *Advanced Powder Technology*, **28**(2): 575–583, 2017, doi: 10.1016/j.apt.2016.10.026.

13. Ciarletta M., Straughan B., Uniqueness and structural stability for the Cattaneo-Christov equations, *Mechanics Research Communications*, **37**(5): 445–447, 2010, doi: 10.1016/j.mechrescom.2010.06.002.

14. Tibullo V., Zampoli V., A uniqueness result for the Cattaneo-Christov heat conduction model applied to incompressible fluids, *Mechanics Research Communications*, **38**(1): 77–79, 2011, doi: 10.1016/j.mechrescom.2010.10.008.

15. Raju C.S.K., Sandeep N., Unsteady three-dimensional flow of Casson-Carreau fluids past a stretching surface, *Alexandria Engineering Journal*, **55**(2): 1115–1126, 2016, doi: 10.1016/j.aej.2016.03.023.

16. Srinivas S., Gayathri R., Kothandapani M., The influence of slip conditions, wall properties and heat transfer on MHD peristaltic transport, *Computer Physics Communications*, **180**(11): 2115–2122, 2009, doi: 10.1016/j.cpc.2009.06.015.

17. Sivasankaran S., Ho C.J., Effect of temperature dependent properties on MHD convection of water near its density maximum in a square cavity, *International Journal of Thermal Sciences*, **47**(9): 1184–1194, 2008, doi: 10.1016/j.ijthermalsci.2007.10.001.

18. Waqas M., Farooq M., Khan M.I., Alsaedi A., Hayat T., Yasmeen T., Magnetohydrodynamic (MHD) mixed convection flow of micropolar liquid due to nonlinear stretched sheet with convective condition, *International Journal of Heat and Mass Transfer*, **102**: 766–772, 2016, doi: 10.1016/j.ijheatmasstransfer.2016.05.142.

19. Hsiao K.L., MHD mixed convection for viscoelastic fluid past a porous wedge, *International Journal of Non-Linear Mechanics*, **46**(1): 1–8, 2011, doi: 10.1016/j.ijnonlinmec.2010.06.005.

20. Srinivas S., Kothandapani M., The influence of heat and mass transfer on MHD peristaltic flow through a porous space with compliant walls, *Applied Mathematics and Computation*, **213**(1): 197–208, 2009, doi: 10.1016/j.amc.2009.02.054.

21. Mahmoud M.A.A., Thermal radiation effects on MHD flow of a micropolar fluid over a stretching surface with variable thermal conductivity, *Physica A: Statistical Mechanics and its Applications*, **375**(2): 401–410, 2007, doi: 10.1016/j.physa.2006.09.010.

22. Ishak A., Nazar R., Pop I., Magnetohydrodynamic (MHD) flow of a micropolar fluid towards a stagnation point on a vertical surface, *Computers & Mathematics with Applications*, **56**(12): 3188–3194, 2008, doi: 10.1016/j.camwa.2008.09.013.

23. Prasad P.D., Saleem S., Varma S.V.K., Raju C.S.K., Three dimensional slip flow of a chemically reacting Casson fluid flowing over a porous slender sheet with a non-uniform heat source or sink, *Journal of the Korean Physical Society*, **74**: 855–864, 2019, doi: 10.3938/jkps.74.855.

24. Tamoor M., Waqas M., Khan M.I., Alsaedi A., Hayat T., Magnetohydrodynamic flow of Casson fluid over a stretching cylinder, *Results in Physics*, **7**: 498–502, 2017, doi: 10.1016/j.rinp.2017.01.005.

25. Upadhya S.M., Mahesha, Raju C.S.K., Shehzad S.A., Abbasi F.M., Flow of Eyring-Powell dusty fluid in a deferment of aluminum and ferrous oxide nanoparticles with Cattaneo-Christov heat flux, *Powder Technology*, **340**: 68–76, 2018, doi: 10.1016/j.powtec.2018.09.015.

26. Lakshmi K.S., Sarojamma G., Makinde O.D., Dual stratification on the Darcy-Forchheimer flow of a Maxwell nanofluid over a stretching surface, *Defect and Diffusion Forum*, **387**: 207–217, 2018, doi: 10.4028/www.scientific.net/DDF.387.207.

27. Kumar S.G., Varma S.V.K., Prasad P.D., Raju C.S.K., Makinde O.D., Sharma R., MHD reacting and radiating 3-D flow of Maxwell fluid past a stretching sheet

with heat source/sink and Soret effects in a porous medium, *Defect and Diffusion Forum*, **387**: 145–156, 2018, doi: 10.4028/www.scientific.net/DDF.387.145.

28. Ullah I., Alkanhal T.A., Shafie S., Nisar K.S., Khan I., Makinde O.D., MHD slip flow of Casson fluid along a nonlinear permeable stretching cylinder saturated in a porous medium with chemical reaction, viscous dissipation, and heat generation/absorption, *Symmetry*, **11**(4): 531 (27 pages), 2019, doi: 10.3390/sym11040531.

29. Mamatha S.U., Raju C.S.K., Prasad P.D., Ajmath K.A., Makinde O.D., Exponentially decaying heat source on MHD tangent hyperbolic two-phase flows over a flat surface with convective conditions, *Defect and Diffusion Forum*, **387**: 286–295, 2018, doi: 10.4028/www.scientific.net/DDF.387.286.

30. Sharma P.R., Choudhary S., Makinde O.D., MHD slip flow and heat transfer over an exponentially stretching permeable sheet embedded in a porous medium with heat source, *Frontiers in Heat and Mass Transfer*, **9**: 1–7, 2017, doi: 10.5098/hmt.9.18.

31. Makinde O.D., Nagendramma V., Raju C.S.K., Leelarathnam A., Effects of Cattaneo-Christov heat flux on Casson nanofluid flow past a stretching cylinder, *Defect and Diffusion Forum*, **378**: 28–38, 2017, doi: 10.4028/www.scientific.net/DDF.378.28.

Received September 22, 2019; accepted version May 18, 2020.
